Site dependence and peak assignment of $YBa_2Cu_3O_{7-x}$ O *K*-edge electron energy loss near-edge fine structure

Teruyasu Mizoguchi,[1] Maria Varela,[2] James P. Buban,[1] Takahisa Yamamoto,[3] and Yuichi Ikuhara[1]
[1]*Institute of Engineering Innovation, The University of Tokyo, 2-11-16, Yayoi, Bunkyo, Tokyo 113-8656, Japan*
[2]*Materials Science & Technology Division, Oak Ridge National Laboratory, Building 3025 M, MS 6030, P.O. Box 2008, Oak Ridge, Tennessee 37831, USA*
[3]*Department of Advanced Materials Science, 5-1-5, The University of Tokyo, Kashiwanoha, Kashiwa, Chiba 277-8561, Japan*
(Received 11 July 2007; revised manuscript received 30 October 2007; published 9 January 2008)

The different peaks in the O *K*-edge near-edge fine structure of $YBa_2Cu_3O_{7-x}$ are interpreted here by using overlap population diagram. This study identifies the peaks in the spectrum as follows: (1) the first peak purely originates from O-Cu interactions, (2) the contributions from Y, Ba, and Cu are comparable at the second and third peaks, (3) and the fourth peak has the largest O-Cu interactions. Therefore, the first and/or fourth peaks and second and/or third peaks can be sensitive to the changes in the atomic and electronic structure at Cu and Y/Ba sites, respectively. The spectral differences depending on the atomic site are also discussed.

DOI: 10.1103/PhysRevB.77.024504 PACS number(s): 74.25.Jb, 79.20.Uv

I. INTRODUCTION

$YBa_2Cu_3O_{7-x}$ (YBCO) is one of the most prominent members of the high temperature superconductive oxides and promising for commercial applications. Since its discovery in 1987, our understanding of superconductivity in cuprates has improved, although the underlying mechanism remains unclear. It is widely accepted, though, that hole states at the top of the valence band are strongly linked with the superconductive properties.[1–5] The oxygen *K* near-edge structures observed by x-ray sources [x-ray appearance near-edge structure (XANES)] and that by using electron energy loss near-edge structure (ELNES) spectroscopy have been widely used in YBCO studies because the intensity of their first peak is proportional to the hole concentration.[6,7] On the other hand, contrary to the first peak, the nature and subsequent assignment of the other peaks in the higher energy loss region have not been clarified so far. Since the wave functions giving rise to the higher energy peaks are generally more delocalized than the ones responsible for the appearance of the first peak, they can be more sensitive to changes in the local atomic and electronic structures. Actually, Batson *et al.* reported O *K* ELNES from carbon doped YBCO and found that not only the first peak but also higher energy peaks are changed by the presence of the dopant.[8] On the other hand, Grigis and Schamm observed the dependence of the spectrum on the oxygen deficiency and reported that no spectral change was found except for the first peak. However, a detailed inspection of this work finds that the higher energy peaks are also affected by the presence of oxygen vacancies.[9] These spectral changes are deeply correlated with changes in the atomic and electronic structures. Therefore, identifying all of the features in the spectrum will enable future spectroscopic studies to gain more insight into the elusive physics of these materials, especially in the new generation aberration corrected electron microscopes which can probe these systems with unprecedented spatial resolutions.[10]

On the other hand, the peak assignments of the ELNES and XANES data are not always straightforward. Partial densities of states (PDOSs) have been widely used to interpret the spectrum. However, the electronic structure of the conduction band of these materials is quite complicated, and PDOS cannot give the bonding information directly. Even when one orbital seems to overlap with another orbital in a PDOS diagram, they sometimes do not have direct bonding with each other in real space. In a previous study of ours, the PDOS was utilized to interpret the O *K* ELNES of YBCO,[11] but the contributions from surrounding cations to some peaks in the spectrum were only qualitatively argued since it was difficult to assign all peaks and obtain bonding information just based on the PDOS diagrams. Here, we go further by using overlap population (OP) diagrams. The OP diagram is sometimes called "crystal orbital overlap population diagram"[12] and has been successfully applied to the detailed analysis of chemical bondings.[13,14] Recently, a combination of band structure calculations with the OP diagram was proposed as a powerful method to interpret the ELNES and XANES of materials.[15] In this paper, we apply the method to YBCO O *K* ELNES and show how the technique constitutes a breakthrough toward unambiguous assignments of the peaks in the spectrum.

II. METHODOLOGY

The ELNES calculation was performed by using an orthogonalized linear combination of atomic orbitals (OLCAO) method within the local density approximation (LDA) of the density functional theory.[16] Although LDA cannot reproduce the antiferromagnetic insulator electronic structure of the ground state of YBCO, it is known that the LDA calculation can successfully reproduce the O *K* ELNES of YBCO except for the position and absolute intensity of the first peak.[11] The OLCAO method was selected because the basis functions are represented by the sum of atomic orbitals. Chemical bonding information, such as PDOS and bond overlap populations (BOP), can be directly obtained in this method. The effect of the core hole, which is generated at a core orbital in the electron transition process, is known to be indispensable to accurately calculate ELNES and XANES.[17–20] As shown in Fig. 1(a), the unit cell of YBCO

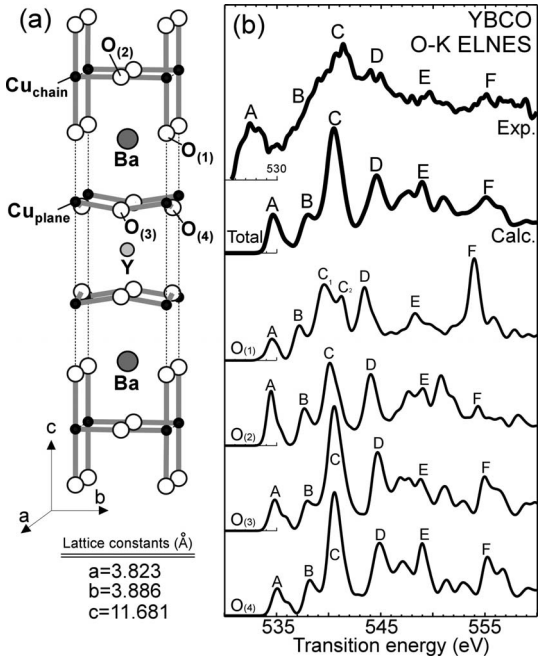

FIG. 1. (a) Atomic structure of YBCO unit cell. (b) (top to bottom) Experimental, calculated O *K* ELNES of YBCO, and calculated O *K* ELNES from individual oxygen site in YBCO. The experimental spectrum was observed with JEOL2010F using Gatan GIF.

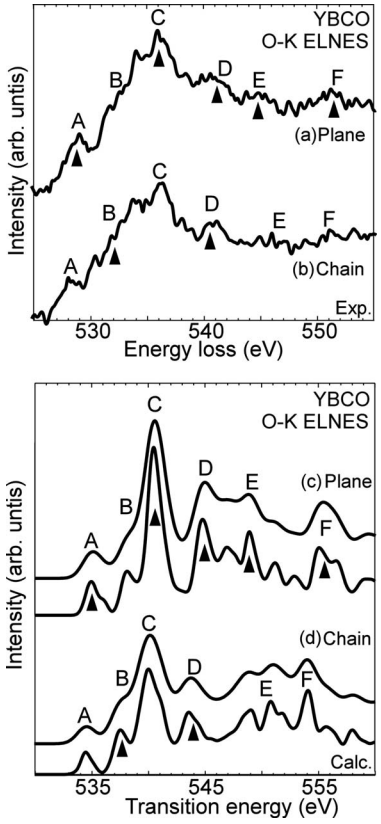

FIG. 2. [(a) and (b)] Experimental O *K* ELNES from the CuO chain (bottom) and CuO_2 plane (top) regions with the electron beam perpendicular to the *c* axis. [(c) and (d)] Calculated O *K* ELNES of the corresponding conditions with two kinds of broadening factors. Arrows represent the spectral differences between the CuO chain and CuO_2 plane.

has several inequivalent O positions: two plane oxygens, $O_{(3)}$ and $O_{(4)}$, one chain oxygen, $O_{(2)}$, and the apical oxygen between the chain and the plane, $O_{(1)}$.[4] Therefore, the core hole was introduced at each site and the spectrum was calculated separately. In order to introduce the core hole accurately, 117 atom supercells were constructed by replicating the YBCO unit cell $3\times3\times1$ times. The OLCAO method is suitable to calculate such large supercell since the core orbitals can be eliminated from the final secular equation by the orthogonalized process.[16] The OP diagram was obtained by calculating the BOP of a pair of atoms at each band. By using the OP diagrams, the peaks in the spectrum can be identified by a combination of bonding and/or antibonding interactions of a pair of atoms. Details on the OP diagram for ELNES and XANES interpretation are described elsewhere.[15,17]

III. RESULTS AND DISCUSSION

A. Site dependence of $YBa_2Cu_3O_7$ O *K* electron energy loss near-edge structure

Figure 1(b) shows the experimental and calculated O *K* ELNES of YBCO. As reported previously, each oxygen site has different spectral features. For example, peak C of $O_{(1)}$ is split to C_1 and C_2 and peak F shows a high intensity. Also, peak A of $O_{(2)}$, peak C of $O_{(3)}$ and $O_{(4)}$, and peak E of $O_{(4)}$ are distinct to those of other sites.[11] In order to compare with the experimental spectrum, the calculated spectra were summed with a weight considering the number of sites contained in the unit cell. The experimental spectrum was obtained with a 2 nm wide electron probe and thus the site dependence, as can be seen in Fig. 2, could not be detected. Error in the transition energy is about 5.0 eV which is less than 1% of the absolute transition energy. It can be seen that the total calculated spectrum well reproduces the experimental spectrum, except for the position of peak A. Peak A originates from the interactions between O $2p$ and partially occupied Cu d orbital.[11] For the quantitative reproduction of peak A, effects of strong electron-electron correlations, such as Mott-Hubbard term $+U$, are necessarily included in the calculation.[21]

In order to detect the site dependence of O *K* ELNES, a smaller electron probe than the unit cell of YBCO, at least subnanometer, is necessary. Recently, electron probes with diameters in the subnanometer order can be obtained owing to the success of aberration correction for scanning transmission electron microscopy (STEM). Figure 2 shows spectra obtained in a VG Microscopes HB501 UX equipped with a Nion aberration corrector and a Gatan Enfina spectrometer. A probe forming aperture of approximately 20 mrad and a detector semiangle of about 12 mrad were used. This microscope and the observation condition can routinely achieve an electron beam with a diameter around 0.13 nm or less. It should be mentioned that the actual resolution of electron energy loss spectroscopy could be worse than the probe size

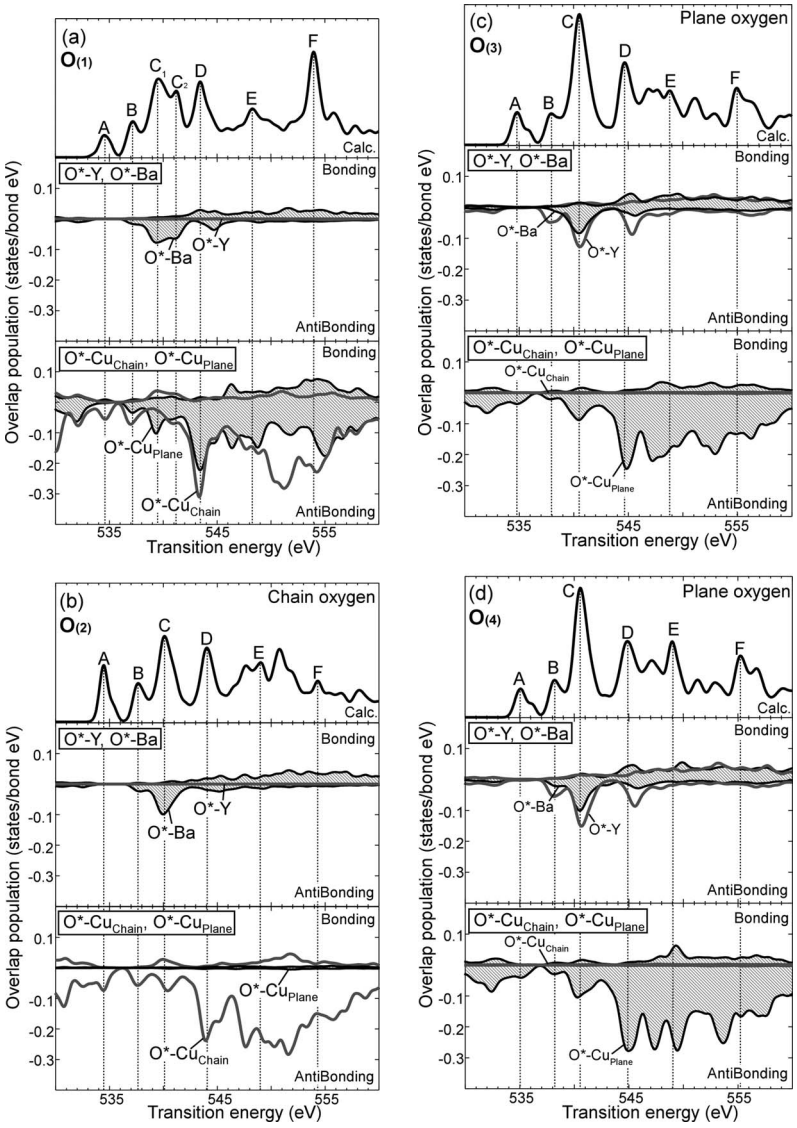

FIG. 3. [(a) to (d)] Calculated O *K* ELNES, the overlap population diagrams for O^*-Ba/O^*-Y, and O^*-Cu_{chain}/O^*-Cu_{plane} for $O_{(1)}$, $O_{(2)}$, $O_{(3)}$, and $O_{(4)}$. The asterisk represents the oxygen which has the core hole at 1*s* core orbital.

because of some delocalization of the incident probe.[22] However, the chain and plane regions in YBCO are over 0.4 nm apart from each other. The recent results reported by Oxley *et al.*, which were obtained in the same machine and under similar observation conditions, proved that the 0.4 nm separation can be readily resolved by the present machine and experimental conditions.[22]

The spectra shown in Fig. 2 were collected from chain and plane regions within an area of an YBCO specimen. It is found that those spectra are different from that observed with 2 nm electron probe (Fig. 1). By comparison with the spectrum in Fig. 1, the separation of peaks D and E is smaller and peak A is less notable at CuO_2 plane region, and the "camel-back" profile is missing and peak B is more notable at the CuO chain region. It is also found that the O *K* ELNES from the CuO chain region and CuO_2 plane region are different from each other: Peaks A have a higher relative intensity, peaks D and E form camel-back profile, and clear peak F appears at the CuO_2 plane region, whereas the CuO chain region shows the higher intensity of peak B and broader profiles from peak A to C and from peak E to F. In addition, a detailed inspection can find that peak A of the CuO_2 plane region is slightly higher energy than the corresponding one from the CuO chain region.

The calculated spectra were also shown in the same figure with two kinds of broadening factor. They were obtained by summing the individual spectra of $O_{(1)}$ and $O_{(2)}$ for the CuO chain region and those of $O_{(3)}$ and $O_{(4)}$ for the CuO_2 plane region. Since the ELNES profile changes with the direction of the momentum transfer vector in relation to that of the crystal orientation,[11,18,23,24] the calculated spectra perpendicular and parallel to the *c* axis are summed under the condition of the equipments. The ratio perpendicular to parallel to the *c* axis (=6:4) was obtained from previous reports.[23,24] It can be seen that the present LDA calculation satisfactorily reproduces the characteristic features in experiment, such as the camel-back profile and the intense peak C at the CuO_2 plane region, and the broad profiles of A–C and E–F at the CuO chain region. As for the trend observed at peak A shift, peak A of the CuO_2 plane region appears at a slightly higher energy than that of the CuO chain region. This trend is also reproduced. It should be mentioned again that a quantitative

reproduction of peak A cannot be obtained by the LDA calculation because the antiferromagnetic insulator electronic structure of YBCO is not reproduced. However, those results in Figs. 1 and 2 indicate that qualitative discussion on peak A is possible by the LDA calculation.

B. Peak assignment of $YBa_2Cu_3O_7$ O *K* electron energy loss near-edge structure

OP diagrams between the core-holed oxygens (O^*) and the surrounding cations are shown in Fig. 3. It should be mentioned that the correlations between peaks in ELNES and the OPs should not be proportional because not only PDOS but also electron transition probability also contribute to the ELNES, whereas the electron transition probability is not considered in the OP diagram. In this study, in order to know the PDOS part, namely, orbital-orbital interactions, at each peak, the OP diagrams were directly compared with the ELNES. Concerning the Y and Ba contributions [middle panels of Fig. 3], it is found for all the oxygen sites that peak A does not have any contributions from the Y and Ba bands. On the other hand, the largest Y and/or Ba contributions appear at peak C. In addition, it is clearly seen that $O_{(1)}$ and $O_{(2)}$ do not have interactions with Y, whereas the CuO_2 plane oxygens $O_{(3)}$ and $O_{(4)}$ interact with both Y and Ba. This can be ascribed to the longer bond length of $O_{(1)}$-Y and $O_{(2)}$-Y, further than 4 Å. In the previous study, it was concluded that peak C of all oxygen sites are mainly caused by the O^*-Ba interaction by using the PDOS diagrams.[11] These OP diagrams, however, reveal that O^*-Y antibonding in the CuO_2 plane oxygens $O_{(3)}$ and $O_{(4)}$ is larger than O^*-Ba antibonding.

Concerning O^*-Cu interactions [bottom panels of Fig. 3], it can be seen that O^*-Cu interactions contribute to all peaks, with the largest O^*-Cu antibonding interactions appearing at peak D of all oxygen sites. By only looking at the PDOS, it was difficult to find which Cu contributes to each oxygen site since the PDOS of both Cu_{chain} and Cu_{plane} overlap in the whole energy region.[11] From the OP diagrams, it is clearly seen that the O^*-Cu_{chain} and O^*-Cu_{plane} antibonding interactions are respectively dominant in the CuO chain oxygen $O_{(2)}$ [Fig. 3(b)], and the CuO_2 plane oxygens $O_{(3)}$ and $O_{(4)}$ [Figs. 3(c) and 3(d)] and both the Cu_{chain} and Cu_{plane} contribute to $O_{(1)}$ [Fig. 3(a)]. Here, it should be mentioned that peak A of $O_{(1)}$ mainly originates from O^*-Cu_{chain} antibonding states, whereas the contribution from the Cu_{plane} is almost negligible, though both Cu_{chain} and Cu_{plane} contribute to other peaks in higher energy region [Fig. 3(a)]. This can be ascribed to the different bond lengths and the character of responsible orbitals for the peaks. That is, $O_{(1)}$-Cu_{plane} (2.35 Å) is longer than that of $O_{(1)}$-Cu_{chain} (1.85 Å), and the Cu 3*d* orbital, which is responsible for peak A, is more localized than Cu 4*s*,*p*,*d* orbitals, which are responsible for the other higher energy peaks. The localized 3*d* orbital of Cu_{plane} cannot have strong interactions with $O_{(1)}$ site, located slightly further away, whereas the effect of Cu_{plane} 4*s*,*p*,*d* orbitals can reach to $O_{(1)}$ site since they are more delocalized than Cu_{plane} 3*d* orbital.

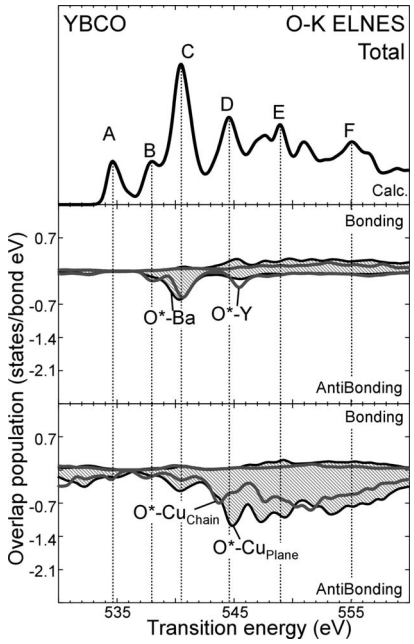

FIG. 4. (top to bottom) Calculated O *K* ELNES of YBCO and the overlap population diagrams for O^*-Ba/O^*-Y and O^*Cu_{chain}/O^*-Cu_{plane} obtained by summing that of individual oxygen with a weight of number of each atom in unit cell. The asterisk represents the oxygen which has the core hole at 1*s* core orbital.

By using those OP diagrams, the causes of the spectral differences depending on the oxygen site can be understood as follows. From the OP diagram of $O_{(1)}$, the contributions of O^*-Cu_{chain} and O^*-Cu_{plane} are found to be different at peaks C_1 and C_2. The difference is considered to be the cause of the splitting of peak C of $O_{(1)}$ [Fig. 3(a)]. Concerning the distinct peaks, i.e., peak F of $O_{(1)}$, peak A of $O_{(2)}$, peak C of $O_{(3)}$ and $O_{(4)}$, and peak E of $O_{(4)}$, it is found that O^*-Cu antibonding interactions at peak A of $O_{(2)}$ and peak E of $O_{(4)}$ are larger than that of other oxygens [Figs. 3(b) and 3(d)]. In addition, from Figs. 3(a)–3(d), it is found that peak F of $O_{(1)}$ and peak C of $O_{(3)}$ and $O_{(4)}$ are composed of two kinds of O^*-cations interactions. Namely, both O^*-Cu_{plane} and O^*-Cu_{chain} interactions contribute to peak F of $O_{(1)}$ and both O^*-Ba and O^*-Y interactions contribute to peak C of $O_{(3)}$ and $O_{(4)}$. Thus, the presences of the larger interactions and multi-O^*-cations interactions are considered to be a cause of those distinct peaks.

IV. SUMMARY

As a summary, Fig. 4 shows the total OP diagrams obtained by summing those of individual oxygen sites with a weight of the number of each site found in the unit cell. From the OP diagrams, the peaks in the YBCO O *K* ELNES are interpreted to be as follows. (1) The contributions of Y and Ba are almost negligible at peak A. (2) Peaks B and C are composed of all O^*-Cu, O^*-Y, and O^*-Ba interactions. (3) The largest O^*-Cu interactions appear at peak D. The higher energy peaks than peak D are mainly caused by the

O^*-Cu antibonding interactions. Those assignments suggest that the first and fourth peaks and the second and third peaks can be sensitive to the atomic and electronic structure changes at the Cu and Y/Ba sites, respectively.

Finally, as we demonstrated above, it is recently possible to collect ELNES from subnano regions owing to the developments of spherical aberration corrector for STEM.[25,26] Such high spatial resolution spectroscopy can be extended to more challenging systems such as interfaces, defects, dislocations, etc. For example, Klie *et al.* applied the ultrahigh resolution analysis to YBCO dislocation and elucidated the dopant segregation mechanisms and the hole concentrations at Ca-doped dislocation cores.[27] The method of peak assignment demonstrated in this study can be utilized for further understanding of such doped and also deficient systems. By giving assignments to those spectra, it is expected that not only the hole concentration but also the local atomic and electronic structure changes can be unraveled.

ACKNOWLEDGMENTS

We give thanks to W. Y. Ching at the University of Missouri-Kansas City for allowing us to use the OLCAO code. Part of this study is supported by The Murata Science Foundation (A61148) and a Grant-in-Aid for Scientific Research in Priority Area "Nano Materials Science for Atomic Scale Modification" from the Ministry of Education, Sports, and Culture of Japan. Work at ORNL is supported by the Office of Basic Energy Sciences, Division of Materials Sciences and Engineering, U.S. DOE, under Contract No. DEAC05-00OR22725 with ORNL, managed and operated by UT Battelle, LLC.

[1] M. K. Wu, J. R. Ashburn, C. J. Torng, P. H. Hor, R. L. Meng, L. Gao, Z. J. Huang, Y. Q. Wang, and C. W. Chu, Phys. Rev. Lett. **58**, 908 (1987).
[2] W. I. F. David, W. T. A. Harrison, J. M. F. Gunn, O. Moze, A. K. Soper, P. Day, J. D. Jorgensen, D. G. Hinks, M. A. Beno, L. Soderholm, D. W. Capone, I. K. Schuller, C. U. Segre, K. Zhang, and J. D. Grace, Nature (London) **327**, 310 (1987).
[3] V. J. Emery, Phys. Rev. Lett. **58**, 2794 (1987).
[4] M. A. Beno, L. Soderholm, D. W. Capone, D. G. Hinks, J. J. Jorgensen, J. D. Grace, and Ivan K. Schuller, Appl. Phys. Lett. **51**, 57 (1987).
[5] P. W. Anderson, Science **235**, 1196 (1987).
[6] J. A. Yarmoff, D. R. Clarke, W. Drube, U. O. Karlsson, A. Taleb-Ibrahimi, and F. J. Himpsel, Phys. Rev. B **36**, 3967 (1987).
[7] N. Nücker, J. Fink, J. C. Fuggle, P. J. Durham, and W. M. Temmerman, Phys. Rev. B **37**, 5158 (1988).
[8] P. E. Batson, T. M. Shaw, D. Dimos, and P. R. Duncombe, Phys. Rev. B **43**, 6236 (1991).
[9] CH. Grigis and S. Schamm, Ultramicroscopy **74**, 159 (1998). Figure 4 of this reference reported the dependence of O *K* ELNES on the oxygen vacancy concentration. Not only the first peak, around 528–530 eV, but also the higher energy peak, around 532–536 eV, changes with the increase of the oxygen vacancy.
[10] M. Varela, A. R. Lupini, K. van Benthem, A. Y. Borisevich, M. C. Chisholm, N. Shibata, E. Abe, and S. J. Pennycook, Annu. Rev. Mater. Res. **35**, 539 (2005).
[11] T. Mizoguchi, J. P. Buban, K. Matsunaga, T. Yamamoto, and Y. Ikuhara, Ultramicroscopy **106**, 92 (2006).
[12] R. Hoffmann, Angew. Chem., Int. Ed. Engl. **26**, 846 (1987).
[13] M. Mizuno, I. Tanaka, and H. Adachi, Phys. Rev. B **59**, 15033 (1999).
[14] T. Mizoguchi, T. Sasaki, S. Tanaka, K. Matsunaga, T. Yamamoto, M. Kohyama, and Y. Ikuhara, Phys. Rev. B **74**, 235408 (2006).
[15] T. Mizoguchi, K. Tatsumi, and I. Tanaka, Ultramicroscopy **106**, 1120 (2006).
[16] W. Y. Ching, J. Am. Ceram. Soc. **73**, 3135 (1990).
[17] T. Mizoguchi, I. Tanaka, M. Yoshiya, F. Oba, K. Ogasawara, and H. Adachi, Phys. Rev. B **61**, 2180 (2000).
[18] T. Mizoguchi, I. Tanaka, S. Yoshioka, M. Kunisu, T. Yamamoto, and W. Y. Ching, Phys. Rev. B **70**, 045103 (2004).
[19] I. Tanaka, T. Mizoguchi, and T. Yamamoto, J. Am. Ceram. Soc. **88**, 2013 (2005).
[20] T. Yamamoto, T. Mizoguchi, and I. Tanaka, Phys. Rev. B **71**, 245113 (2005).
[21] P. Novák, F. Boucher, P. Gressier, P. Blaha, and K. Schwarz, Phys. Rev. B **63**, 235114 (2001).
[22] M. P. Oxley, M. Varela, T. J. Pennycook, K. van Benthem, S. D. Findlay, A. J. D'Alfonso, L. J. Allen, and S. J. Pennycook, Phys. Rev. B **76**, 064303 (2007).
[23] N. D. Browning, J. Yuan, and L. M. Brown, Ultramicroscopy **38**, 291 (1991).
[24] R. Klie, H. Su, Y. Zhu, J. Davenport, J. Idrobo, and N. Browning, and P. Nellist, Phys. Rev. B **67**, 144508 (2003).
[25] M. Varela, S. D. Findlay, A. R. Lupini, H. M. Christen, A. Y. Borisevich, N. Dellby, O. L. Krivanek, P. D. Nellist, M. P. Oxley, L. J. Allen, and S. J. Pennycook, Phys. Rev. Lett. **92**, 095502 (2004).
[26] H. Ohta, S. W. Kim, Y. Mune, T. Mizoguchi, K. Nomura, S. Ohta, T. Nomura, Y. Nakanishi, Y. Ikuhara, M. Hirano, H. Hosono, and K. Koumoto, Nat. Mater. **6**, 129 (2007).
[27] R. F. Klie, J. P. Buban, M. Varela, A. Franceschetti, C. Jooss, Y. Zhu, N. D. Browning, S. T. Pantelides, and S. J. Pennycook, Nature (London) **435**, 475 (2006).